Langmuir

Article

pubs.acs.org/Langmuir

Stereochemical Effect Revealed in Self-Assemblies Based on Archaeal Lipid Analogues Bearing a Central Five-Membered Carbocycle: A SAXS Study

Alicia Jacquemet,[†,‡] Cristelle Mériadec,[‡,§] Loïc Lemiègre,[*,†,‡] Franck Artzner,[‡,§] and Thierry Benvegnu[†,‡]

[†]Ecole Nationale Supérieure de Chimie de Rennes, CNRS, UMR 6226, Avenue du Général Leclerc, CS 50837, 35708 Rennes Cedex 7, France

[‡]Université Européenne de Bretagne, France

[§]Institut de Physique de Rennes, Université Rennes 1, UMR-CNRS 6251, Campus Beaulieu Bat. 11A, 35042 Rennes Cedex, France

Supporting Information

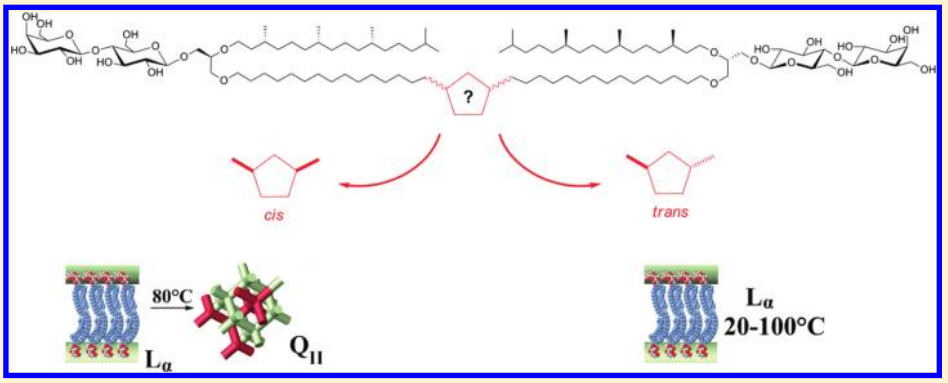

ABSTRACT: The relative stereochemistry (cis or trans) of a 1,3-disubstituted cyclopentane unit in the middle of tetraether archaeal bipolar lipid analogues was found to have a dramatic influence on their supramolecular self-assembly properties. SAXS studies of two synthetic diastereomeric archaeal lipids bearing two lactosyl polar head groups at opposite ends revealed different lyotropic behaviors. The cis isomer led to $L_c-L_\alpha-Q_{II}$ transitions whereas the trans isomer retained an L_α phase from 20 to 100 °C. These main differences originate from the conformational equilibrium (pseudorotation) of 1,3-disubstituted cyclopentanes. Indeed, this pseudorotation exhibits quite similar orientations of the two substituents in a trans isomer whereas several orientations of the two alkyl chains are expected in a *cis*-1,3-dialkyl cyclopentane, thus authorizing more conformational flexibility in the lipid packing.

INTRODUCTION

Even if lipids are the most studied amphiphiles,[1−6] stereochemical issues are still not fully understood. The main reason is based on the fact that most of the lipids originating from mesophile organisms bear linear or unsaturated alkyl chains devoid of stereogenic centers. However, some organisms such as archaea commonly involve lipids that include numerous stereogenic centers in their hydrophobic domain. One of the most remarkable archaeal lipids is characterized by a bipolar structure based on a tetraether diglyceryl backbone (Figure 1).[7−9] Physicochemical studies have been performed on both natural lipids and synthetic analogues; however, the role of the 1,3-disubstituted cyclopentyl rings, for instance, remains unclear.[10,11]

As part of an ongoing research program that involved the synthesis of archaeal lipid analogues[12,13] and the demonstration of their possible applications,[14−16] we recently published the synthesis and preliminary cryo-TEM comparative studies of the behavior of two identical bipolar lipids except the stereochemistry of their central cyclopentyl unit (Figure 1).[17] These bipolar molecules are characterized by a hydrophobic skeleton constructed around a bridging chain incorporating a central cyclopentane unit. This carbocycle is 1,3-disubtituted by two linear chains that are both terminated by two stereocontrolled glyceryl moieties and two optically pure phytanyl chains. These tetraether structures are further equipped with lactosyl polar headgroups to bring about an adequate hydrophilic/hydrophobic balance. Additionally, the presence of neutral sugar headgroups instead of charged phosphorylated derivatives is expected to provide a higher sensitivity of the self-assembly properties of these glycolipids toward minor changes in their hydrophobic cores such as the stereochemical variations we describe hereafter.[18]

Received: November 22, 2011
Revised: April 21, 2012
Published: April 30, 2012

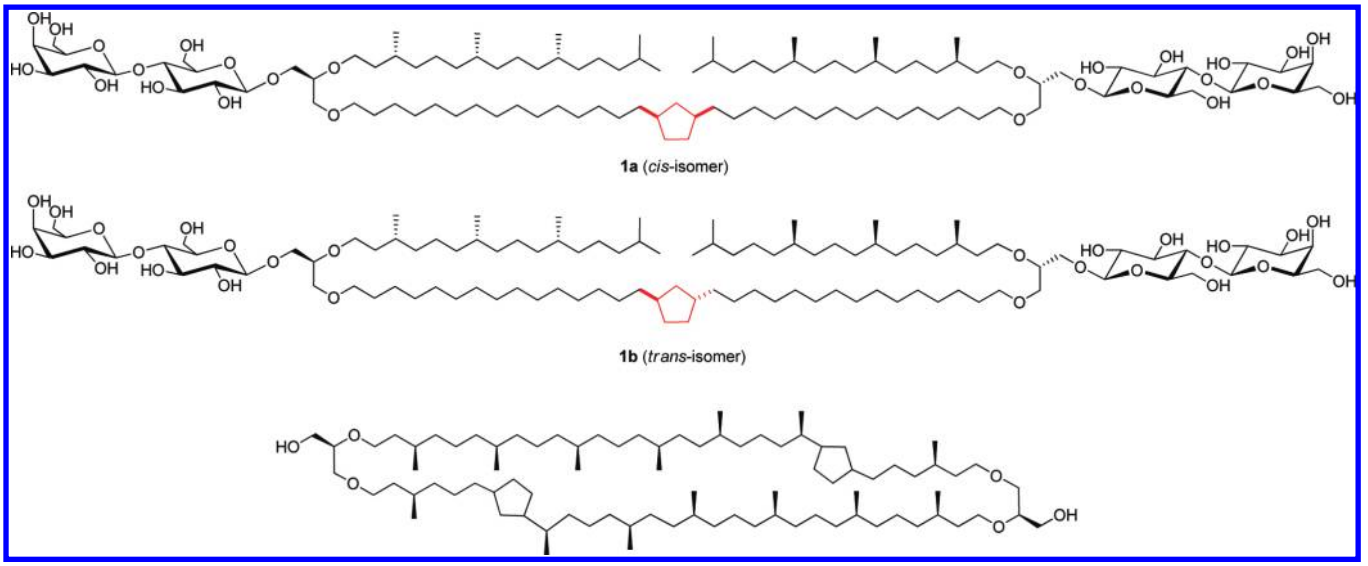

Figure 1. Structure of synthetic archaeal lipid analogues bearing a cis or trans 1,3-disubstituted cyclopentane ring and an example of a tetraether-type archaeal membrane lipid (without a polar headgroup).

The cryo-TEM observation of aqueous solutions of these two diastereoisomers demonstrated the importance of the stereochemistry of the central cyclopentane. Briefly, at the same concentration (1 mg mL^{-1}) and from the same preparation method, the trans isomer showed multilamellar vesicles whereas the cis counterpart led to nonspherical nanoobjects such as lamellae.[17] To gain further insight into the origin of these differences, we describe herein a small-angle X-ray scattering (SAXS) study of the behavior of synthetic tetraethers **1a,b** in concentrated media (50 mg mL^{-1}) and at variable temperatures ranging from 20 to 100 °C.

EXPERIMENTAL SECTION

Sample Preparation. Lipids **1a,b** were prepared following the procedure described previously by our research group.[17] An organic lipid solution (0.1 mL/5 mg in $CHCl_3$/MeOH 2:1) was concentrated under reduced pressure using a rotary evaporator. The corresponding film was dried under high vacuum overnight and hydrated with 0.1 mL of pure water. After 1 night, a vortex/sonication cycle was applied twice to the sample (vortex, sonication (bath, 35 kHz) 2 × 5 min with 5 min between, 25 °C). The corresponding solution was then transferred to a suitable capillary for SAXS experiments.

SAXS Measurements. X-ray scattering experiments were performed using a FR591 Bruker AXS rotating anode X-ray generator operated at 50 kV and 50 mA with monochromatic Cu Kα radiation (λ = 1.541 Å) and point collimation. X-ray patterns were collected with a Mar345 Image-Plate detector (Marresearch, Norderstedt, Germany). The monochromatic Cu Kα radiation (λ = 1.541 Å) was directed with a 350 μm × 350 μm focal spot at 320 mm by double reflection on an elliptical cross multilayer Montel mirror (Incoatec, Geesthacht, Germany). The beam was defined under vacuum by four motorized carbon−tungsten slits (JJ-Xray, Roskilde, Denmark) positioned in front of the mirror (500 μm × 500 μm). Four additional guard slits (600 μm × 600 μm) were placed at the focal point with a 220 mm slit separation distance. The flux after the output mica windows was 3 × 10^8 photons/s. A 2-mm-diameter square lead beam stop was placed under vacuum at 270 mm; afterward, the sample and the detector were positioned at 420 mm. The X-ray patterns were therefore recorded for a range of reciprocal spacings $q = 4\pi(\sin\theta)/\lambda$ from 0.03 to 1.6 $Å^{-1}$, where θ is the diffraction angle. The samples were placed into 1.5 mm glass capillaries (Glas W. Muller, Germany). Acquisition was set to 1 h after a time of 15 min between each temperature. The sequence was repeated twice on each sample.

RESULTS

The comparative behavior of tetraethers **1a,b** in aqueous media was characterized by SAXS experiments. The samples were prepared by the hydration of lipid films at a concentration of around 50 mg mL^{-1}, transferred to a capillary, and studied at variable temperatures (heating and cooling from 20 to 100 °C, 15 min between each temperature, acquisition of 1 h). The heating−cooling sequence was carried out two times without differences. The SAXS patterns obtained for cis isomer **1a** are shown in Figure 2. At 20 and 30 °C, Bragg peaks are clearly

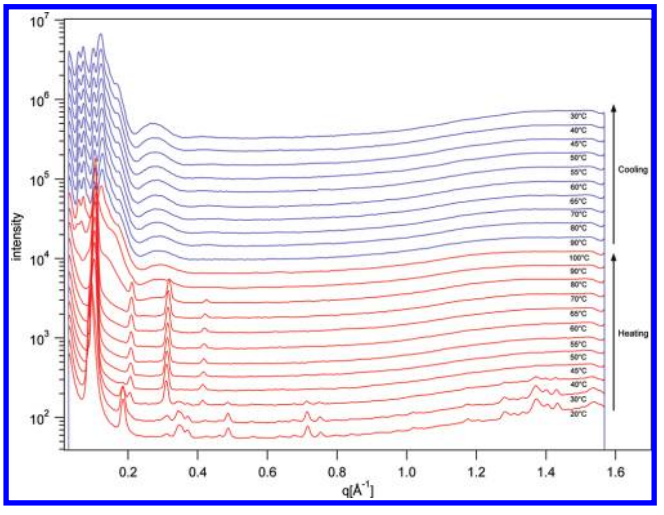

Figure 2. SAXS diagrams corresponding to cis isomer **1a** at variable temperature (20−100 °C).

shown in the smaller-angle region originating from a lamellar phase that exhibits crystalline character as demonstrated by fine Bragg peaks in the WAXS region. The presence of this crystalline state at 20 °C was not expected for lipids including phytanyl chains, which usually provide sufficient fluidity leading to an L_c/L_α transition at lower temperature.[19,20] At 40 °C, an L_α phase (q_1 = 0.103, q_2 = 0.206, q_3 = 0.309, q_4 = 0.413 $Å^{-1}$, d = 61 Å) appeared in coexistence with the L_c phase and became the sole visible phase at 45 °C. It is noteworthy that the d

dx.doi.org/10.1021/la2045948 | Langmuir 2012, 28, 7591−7597

spacing parameter was in accordance with the thickness of the lamellae observed by cryoTEM[17] and the results of Winter et al.[21] obtained from natural archaeal tetraethers. Further increases in the temperature to 80 °C induced a slight decrease in the *d* spacing parameter to 59 Å (80 °C). From this temperature, the system started a new phase transition in favor of a bicontinuous cubic phase (Q) that remained at 100 °C and all along the cooling stage. Several days at 20 °C were needed for the L_α and L_c phases to reappear with the same parameters as those collected during the heating. This type of hysteresis is commonly known for L_α/Q transitions and has been explained recently by Siegel by considering a fourth-order-curvature energy model.[22] The Q phase was identified as a double-diamond-type inverse cubic phase (*Pn*3*m*) by the indexation of the following reflection sequence: $\sqrt{2}$, $\sqrt{3}$, $\sqrt{4}$, $\sqrt{6}$, $\sqrt{9}$, $\sqrt{12}$, $\sqrt{14}$, and $\sqrt{17}$ (Table 1, Figure 3). The *Pn*3*m* space

Table 1. Indexing of the Cubic Phase (*Pn*3*m*) Shown in Figure 3 (*a* = 152 Å)

$(h^2 + k^2 + l^2)^{1/2}$	(*h*, *k*, *l*)	q_{calc} (Å^{-1})	q_{obs} (Å^{-1})
$\sqrt{2}$	(1, 1, 0)	0.0585	0.0588
$\sqrt{3}$	(1, 1, 1)	0.0716	0.0717
$\sqrt{4}$	(2, 0, 0)	0.0827	0.0833
$\sqrt{6}$	(2, 1, 1)	0.1013	0.1014
$\sqrt{9}$	(2, 2, 1)	0.1240	0.1233
$\sqrt{12}$	(2, 2, 2)	0.1432	0.1428
$\sqrt{14}$	(3, 2, 1)	0.1547	0.1544
$\sqrt{17}$	(3, 2, 2)	0.1704	0.1699

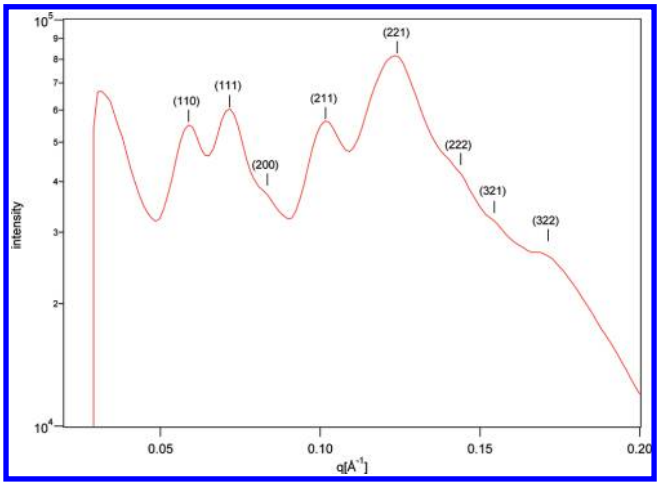

Figure 3. SAXS diagram corresponding to cis isomer **1a** at 100 °C and Q_{II} (*Pn*3*m*) reflection indexation, where the positions of the expected Bragg peaks are indicated by lines and (*hkl*).

group was assigned without any ambiguity; neither the *Ia*3*d* nor the *Im*3*m* space groups were compatible with these reflection ratios because they would involve different reflection patterns (*Ia*3*d*: $\sqrt{6}$, $\sqrt{8}$, $\sqrt{14}$, $\sqrt{16}$, and $\sqrt{20}$. Im3m: $\sqrt{2}$, $\sqrt{4}$, $\sqrt{6}$, $\sqrt{8}$, $\sqrt{10}$, $\sqrt{12}$, and $\sqrt{14}$). Consequently, tracing q_{hkl} in $(h^2 + k^2 + l^2)^{1/2}$, where *h*, *k*, and *l* refer to Miller indices, gave access to a repeating parameter of 152 Å for this cubic phase (*Pn*3*m*) (details in the Supporting Information (SI)).[23]

The accuracy of the SAXS pattern allowed the calculation of the electron density profile of the lamellar α phase (L_α) from the four Bragg reflections q_1, q_2, q_3, and q_4. From the eight possible electron density profiles, we selected the electron density profiles shown in Figure 4 (L_α) from molecular criteria.

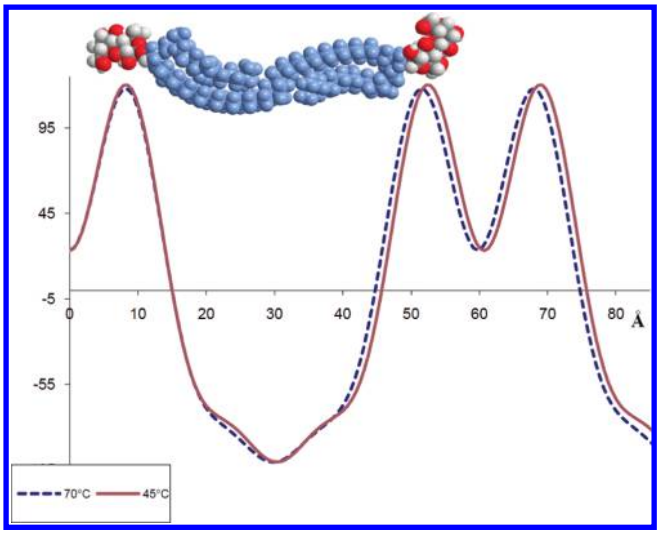

Figure 4. Electron density profile of the L_α phase calculated from the SAXS diagrams of **1a** (45 and 70 °C (heating)).

These electron density profiles calculated at 45 and 70 °C (details in SI) are consistent with a stretched conformation of the tetraether lipid within the L_α phase. The two electron density maxima correspond to the sugar headgroups that are separated by a thin water layer. The headgroup interdistance (17 Å) does not change with the temperature. The aliphatic chains region exhibits a lower electron density without a sharp minimum, which is normally observed in conventional glycolipids.[24] This is in agreement with the bipolar chemical structure. Upon heating, the aliphatic chains slightly decrease from 30.5 to 29.5 Å.

The SAXS data for the Q_{II} phase have also been examined in more detail with respect to the geometrical model of the minimal surfaces.[25,26] The aliphatic chain thickness (16 Å) is expected to be similar in both cubic and lamellar phases because the chains are located on the minimal surface that exhibits a vanishing curvature. The mean areas per methylene at the headgroup/chain interface (S1) and at the center of the structure (S2) were compared. Although S1 and S2 are equal for the L_α phase (S1 = S2), within the Q_{II} phase this results in an 8% increase in favor of S2. On the molecular scale, this can be interpreted as a slight surface excess of the cyclopentyl that could be at the origin of membranes with a radius of mean curvature of 21 nm. The water content can be calculated from the half length of the molecules (30 Å) and the cubic parameter and is 30% by volume.

The SAXS patterns acquired from trans isomer **1b** are shown in Figure 5. The indexation of the Bragg peaks led to the description of the L_α phase all along the variable temperature study from 20 to 100 °C and during the cooling stage. The consecutive Bragg peaks corresponded to *d* spacing parameters between 63 Å at 20 °C (q_1 = 0.100, q_2 = 0.200, q_3 = 0.300, and q_4 = 0.400 Å^{-1}) and 59 Å at 100 °C (q_1 = 0.107, q_2 = 0.214, q_3 = 0.321, and q_4 = 0.429 Å^{-1}), which were again comparable to what we observed by cryoTEM[17] and the results of Winter et al.[21] obtained from natural archaeal tetraethers. A minor coexisting phase that could not be fully characterized was also visible at 100 °C and during the cooling stage. Attempts to favor the appearance of this phase and to avoid kinetic issues during the SAXS measurements (holding the sample for 20 h at 100 °C) led to the same SAXS diagram. After 6 days at 20 °C, L_α was totally recovered with the same parameters. Another

dx.doi.org/10.1021/la2045948 | *Langmuir* 2012, 28, 7591−7597

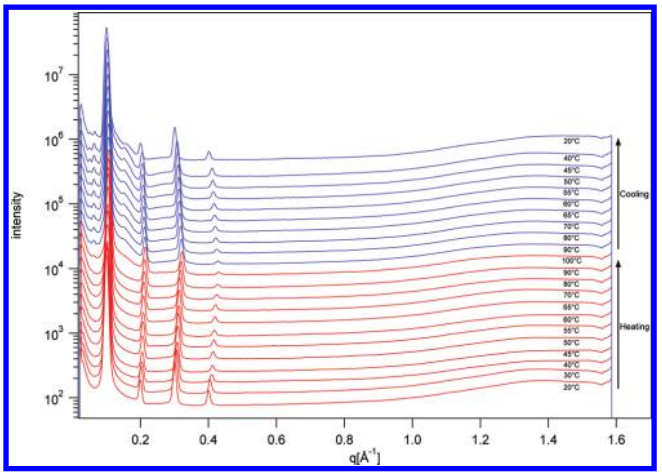

Figure 5. SAXS diagrams corresponding to trans isomer **1b** at variable temperature (20−100 °C).

temperature cycle on the same sample reproduced the same behavior.

The electron density profiles were calculated from the Bragg peak intensity of the L_α phase, and the most adequate profiles at 20, 60, and 100 °C are shown in Figure 6. As for the cis isomer, the electron density profiles are consistent with a stretched conformation of the tetraether within the membrane (L_α phase). Moreover, the polar headgroups are not affected by the temperature, with a constant thickness of 17 Å. The shortening from 32 to 28 Å of the hydrophobic domain according to the temperature increase is, however, well established. It contrasts with the results obtained by Winter et al. showing increasing *d* spacing parameters with increasing temperature when they studied natural archaeal tetraether lipid membranes.[21] This difference may be related to the type of polar headgroups that were on the hydrophobic cores. Indeed, the increasing *d* spacing of the natural tetraether lipid membranes is reported to be due to an increase in hydration at the polar headgroups, which is not observed in our case. The decrease observed for the *d* space of the lipid membrane is clearly due to a shortening of the hydrophobic domain as shown on the electron density profile (Figure 6).

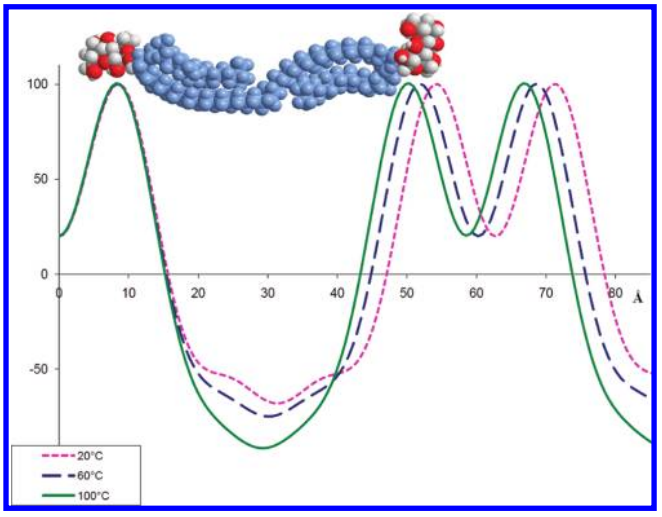

Figure 6. Electron density profile of the L_α phase calculated from the SAXS diagrams of **1b** (20, 60, and 100 °C (heating)).

DISCUSSION

The comparative SAXS studies of the two tetraethers **1a**,**b** bearing cyclopentane rings with opposite relative stereochemistry clearly showed a different temperature dependency of the lyotropic behavior. Indeed, cis isomer **1a** exhibited a crystalline state at 20 °C and needed to be at 40 °C to reach a fluidic state (L_α) whereas trans isomer **1b** behaved as a fluid lamellar phase (L_α) at 20 °C. The unexpected presence of an L_c phase at room temperature and until 40 °C is not fully understood. As mentioned before, the phytanyl chains usually provide an increased fluidic state that induces a decrease in the solid−liquid crystalline phase transition temperature.[19,20] Interestingly, the L_α phases, observed at the beginning of the heating experiment, involved for both isomers a stretched transmembrane conformation (determined from the electron density profiles). Starting from this similar conformation, these L_α phases behave differently during the temperature increase. Indeed, the lamellar phase was stable all along the studied temperature range (20−100 °C) for trans isomer **1b**, but it evolved to a diamond-type bicontinuous cubic phase (*Pn*3*m*) for cis isomer **1a**. The appearance of bicontinuous cubic phases after a temperature increase is well known with other lipids and is roughly related to thermal agitation.[27−30] Indeed, the transition from L_α to Q_{II} (*Pn*3*m*) is known to involve a dramatic change in membrane curvature to fit the requirement of the new phase. However, the absence of a transition from L_α or Q_{II} to the inverse hexagonal phase (H_{II}) reveals an important frustration within the H_{II} phase that is better satisfied within the cubic phase organization (*Pn*3*m*). The criteria that stabilize Q_{II}

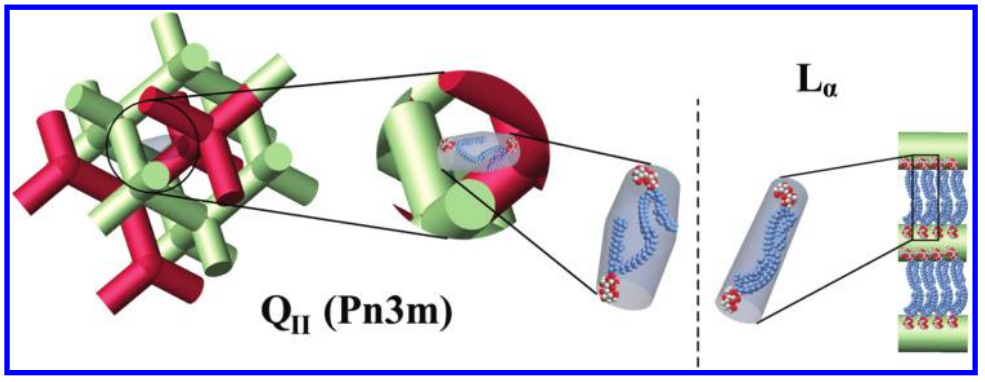

Figure 7. Schematic representation of the volume of tetraether **1a** within the Q_{II} and L_α phases and the chain splay relationship.

dx.doi.org/10.1021/la2045948 | *Langmuir* 2012, 28, 7591−7597

phases are not fully known and are the subject of recent research. The main criteria appear to be the propensity for adequate membrane curvature,[22,29] the chain-packing stress,[31] and the chain splay ability.[28] Hence, in the case of cis isomer **1a** the L_α/Q_{II} transition could be induced by the relative conformational flexibility character of the lipid adopting different conformations within the lipid membrane. This means that even if the electron density profile (L_α) is consistent with a stretched conformation of the cis isomer, the L_α/Q_{II} transition was allowed through a conformational adaptation increasing the membrane curvature and reducing the packing frustration within the Q_{II} phase.[27,31,32] Therefore, the 8% surface increase in the middle of the lipid can be accounted for by a decrease in length, maintaining a constant molecular volume and being compatible with the required shortened length between two perpendicular water networks (Figure 7). This conformational adaptation is explained by a chain splay that occurs only in the case of cis isomer **1a**.

The trans isomer preferentially adopts a unique conformation that is maintained whatever the temperature (20−100 °C), retaining a fluid lamellar phase and inhibiting the transition to other types of phases (Q_{II}, H_{II}). Therefore, this isomer exhibits a poor chain splay ability and a membrane curvature increase that does not fit with the Q_{II} and even less with the H_{II} stabilization criteria.

The structure/property relationships related to the physicochemical observations discussed previously are not obvious. The relatively poor structural differences between tetraethers **1a** and **1b** would suggest similar self-assembly behavior. The geometrical equilibrium of the cyclopentane rings has to be considered to explain the impact of the relative stereochemistry of such cycles. Indeed, cyclopentane is known to adopt numerous conformations of similar energies that originate from the pseudorotation of the carbocycle.[33,34] Following the same conformational pseudorotation, the conformation of 1,3-disubstituted cyclopentane has already been studied by Ruiz del Ballesteros et al.[35] Their results led to rather different energy profiles for the cis and trans isomers all along the pseudorotation circuit. The less-energetic conformation of the cis isomer corresponds to an envelope placing the two methyl groups at a pseudoequatorial position, and for the trans isomer, the less-energetic conformer is a half-chair. These more stable conformations correspond to the greatest distance between the two carbon atoms of the substituents (Me) for both isomers (4.8 Å). Interestingly, far from these more stable conformations, the pseudorotation of the cis isomer results in conformers that place the two methyl groups at distances of 4.8−3.2 Å.[35] Conversely, within a similar energy range (6 kcal mol^{-1}) the pseudorotation of the trans isomer keeps the Me−Me distances between 4.8 and 4.5 Å. Therefore, if both isomers are able to adopt different conformations within a narrow range of energy, then the pseudorotation applied to the cis isomer has a much higher impact on the orientation of the two substituents.

Within a tetraether structure (**1a**,**b**), the stretched conformation observed within the lamellar phases for both isomers probably originates from the thermodynamically stable conformations of the cyclopentyl ring. However, the pseudorotation of the *cis*-1,3-disubstituted-cyclopentyl ring induces, for instance, a closeness of the two alkyl chain arms and a large number of gauche defects within these alkyl chains (Figure 8). This results in a conformational change in the tetraether core in favor of a shrunken conformer. The reduction of the tetraether length is then balanced by a chain splay and permits the fitting

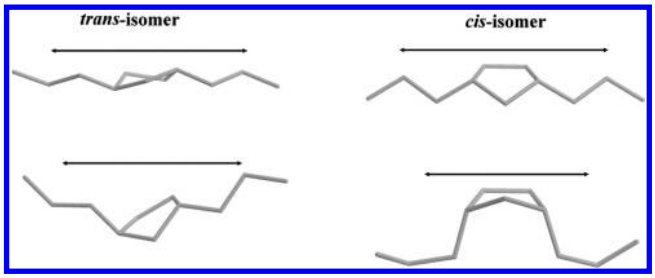

Figure 8. Representative conformations obtained by the pseudorotation of cyclopentane rings bearing 1,3-alkyl chains.

of the membrane curvature needed for the transition to the Q_{II} phase. Conversely, within trans isomer **1b**, the poor effect of the cyclopentane pseudorotation on the orientation of the alkyl chains leads to less flexibility whatever the local conformation of the cyclopentane ring, preventing any chain splay or membrane curvature increase. Thus, the lamellar structure (L_α) undergoes an increase in cohesion, and transitions to other types of phases are avoided or require higher temperatures.

■ CONCLUSIONS

The comparison of the two sets of data obtained from the SAXS studies demonstrates the remarkable influence of the stereochemistry of a tetraether-type lipid structure (archaeal lipid analogues). The sole change in the relative stereochemistry of a cyclopentane ring placed in the middle of a 35 carbon atom chain induces dramatic changes in the lyotropic behavior of such bipolar lipids. Indeed, the cis isomer gathers some of the required criteria stabilizing a Q_{II} phase, and the trans isomer reveals a lack of flexibility in avoiding the phase transition from the original L_α phase. Our study suggests that the energetically low pseudorotation of a *trans*-1,3-dialkyl cyclopentane ring has a limited effect on alkyl chain orientations and even permits a more cohesive lamellar membrane. Indeed, compared to the cis isomer, the *trans*-1,3-cyclopentyl ring permits at least a shift in the lamellar/nonlamellar transitions to higher temperatures in the case of the lipids studied here. This work would influence the design of such bipolar lipids for their use in technical or biotechnical applications in which cubic bicontinuous phases provide smart and useful nanostructures.[36−42] However, because the placement and the number of cyclopentane rings are different in the present analogues, additional studies are still required to explain the presence of *trans*-1,3-disubstituted cyclopentyl rings rather than cis counterparts in archaeal lipids.

■ ASSOCIATED CONTENT

Ⓢ Supporting Information

Details of the determination of the electron density profiles and the lattice parameters. This material is available free of charge via the Internet at http://pubs.acs.org.

■ AUTHOR INFORMATION

Corresponding Author

*E-mail: loic.lemiegre@ensc-rennes.fr.

Notes

The authors declare no competing financial interest.

■ ACKNOWLEDGMENTS

The Agence Nationale de la Recherche (ANR-09-JCJC-0034) and the Région Bretagne are gratefully and respectively acknowledged for financial support and a Ph.D. grant to A.J.

■ REFERENCES

(1) Shimizu, T.; Masuda, M.; Minamikawa, H. Supramolecular Nanotube Architectures Based on Amphiphilic Molecules. *Chem. Rev.* **2005**, *105*, 1401−1444.
(2) Bhattacharya, S.; Biswas, J. Understanding Membranes through the Molecular Design of Lipids. *Langmuir* **2010**, *26*, 4642−4654.
(3) Menger, F. M.; Shi, L.; Rizvi, S. A. A. Self-Assembling Systems: Mining a Rich Vein. *J. Colloid Interface Sci.* **2010**, *344*, 241−246.
(4) Lee, H. Y.; Nam, S. R.; Hong, J.-I. Self-Assembled Organic Microtubes from Amphiphilic Molecules. *Chem.—Asian J.* **2009**, *4*, 226−235.
(5) Goodby, J. W.; Gortz, V.; Cowling, S. J.; Mackenzie, G.; Martin, P.; Plusquellec, D.; Benvegnu, T.; Boullanger, P.; Lafont, D.; Queneau, Y.; Chambert, S.; Fitremann, J. Thermotropic Liquid Crystalline Glycolipids. *Chem. Soc. Rev.* **2007**, *36*, 1971−2032.
(6) Binder, W. H.; Barragan, V.; Menger, F. M. Domains and Rafts in Lipid Membranes. *Angew. Chem., Int. Ed.* **2003**, *42*, 5802−5827.
(7) Benvegnu, T.; Brard, M.; Plusquellec, D. Archaeabacteria Bipolar Lipid Analogues: Structure, Synthesis and Lyotropic Properties. *Curr. Opin. Colloid Interface Sci.* **2004**, *8*, 469−479.
(8) Jacquemet, A.; Barbeau, J.; Lemiègre, L.; Benvegnu, T. Archaeal Tetraether Bipolar Lipids: Structure, Function and Applications. *Biochimie* **2009**, *91*, 711−717.
(9) Benvegnu, T.; Lemiègre, L.; Cammas-Marion, S. Archaeal Lipids: Innovative Materials for Biotechnological Applications. *Eur. J. Org. Chem.* **2008**, 4725−4744.
(10) Fuhrhop, J. H.; Wang, T. Bolaamphiphiles. *Chem. Rev.* **2004**, *104*, 2901−2938.
(11) Chong, P. L.-G. Archaebacterial Bipolar Tetraether Lipids: Physico-Chemical and Membrane Properties. *Chem. Phys. Lipids* **2010**, *163*, 253−265.
(12) Brard, M.; Lainé, C.; Réthoré, G.; Laurent, I.; Neveu, C.; Lemiègre, L.; Benvegnu, T. Synthesis of Archaeal Bipolar Lipid Analogues: A Way to Versatile Drug/Gene Delivery Systems. *J. Org. Chem.* **2007**, *72*, 8267−8279.
(13) Brard, M.; Richter, W.; Benvegnu, T.; Plusquellec, D. Synthesis and Supramolecular Assemblies of Bipolar Archaeal Glycolipid Analogues Containing a *cis*-1,3-Disubstituted Cyclopentane Ring. *J. Am. Chem. Soc.* **2004**, *126*, 10003−10012.
(14) Lainé, C.; Mornet, E.; Lemiègre, L.; Montier, T.; Cammas-Marion, S.; Neveu, C.; Carmoy, N.; Lehn, P.; Benvegnu, T. Folate-Equipped Pegylated Archaeal Lipid Derivatives: Synthesis and Transfection Properties. *Chem.—Eur. J.* **2008**, *14*, 8330−8340.
(15) Réthoré, G.; Montier, T.; Le Gall, T.; Delépine, P.; Cammas-Marion, S.; Lemiègre, L.; Lehn, P.; Benvegnu, T. Archaeosomes Based on Synthetic Tetraether-Like Lipids as Novel Versatile Gene Delivery Systems. *Chem. Commun.* **2007**, 2054−2056.
(16) Benvegnu, T.; Réthoré, G.; Brard, M.; Richter, W.; Plusquellec, D. Archaeosomes Based on Novel Synthetic Tetraether-Type Lipids for the Development of Oral Delivery Systems. *Chem. Commun.* **2005**, 5536−5538.
(17) Jacquemet, A.; Lemiègre, L.; Lambert, O.; Benvegnu, T. How the Stereochemistry of a Central Cyclopentyl Ring Influences the Self-Assembling Properties of Archaeal Lipid Analogues: Synthesis and CryoTEM Observations. *J. Org. Chem.* **2011**, *76*, 9738−9747.
(18) Corti, M.; Cantu, L.; Brocca, P.; Del Favero, E. Self-Assembly in Glycolipids. *Curr. Opin. Colloid Interface Sci.* **2007**, *12*, 148−154.
(19) Kitano, T.; Onoue, T.; Yamauchi, K. Archaeal Lipids Forming a Low Energy-Surface on Air-Water Interface. *Chem. Phys. Lipids* **2003**, *126*, 225−232.
(20) Hato, M.; Yamashita, J.; Shiono, M. Aqueous Phase Behavior of Lipids with Isoprenoid Type Hydrophobic Chains. *J. Phys. Chem. B* **2009**, *113*, 10196−10209.
(21) Chong, P. L.-G.; Zein, M.; Khan, T. K.; Winter, R. Structure and Conformation of Bipolar Tetraether Lipid Membranes Derived from Thermoacidophilic Archaeon Sulfolobus Acidocaldarius as Revealed by Small-Angle X-ray Scattering and High-Pressure FT-IR Spectroscopy. *J. Phys. Chem. B* **2003**, *107*, 8694−8700.
(22) Siegel, D. P. Fourth-Order Curvature Energy Model for the Stability of Bicontinuous Inverted Cubic Phases in Amphiphile-Water Systems. *Langmuir* **2010**, *26*, 8673−8683.
(23) Sun, R. G.; Zhang, J. The Cubic Phase of Phosphatidylethanolamine Film by Small Angle X-Ray Scattering. *J. Phys. D: Appl. Phys.* **2004**, *37*, 463−467.
(24) Schneider, M. F.; Zantl, R.; Gege, C.; Schmidt, R. R.; Rappolt, M.; Tanaka, M. Hydrophilic/Hydrophobic Balance Determines Morphology of Glycolipids with Oligolactose Headgroups. *Biophys. J.* **2003**, *84*, 306−313.
(25) Turner, D. C.; Wang, Z.-G.; Gruner, S. M.; Mannock, D. A.; McElhaney, R. N. Structural Study of the Inverted Cubic Phases of Di-Dodecyl Alkyl-B-D-Glucopyranosyl-Rac-Glycerol. *J. Phys. II* **1992**, *2*, 2039−2063.
(26) Vittorio, L. Polymorphism of Lipid-Water Systems: Epitaxial Relationships, Area-Per-Volume Ratios, Polar-Apolar Partition. *J. Phys. II* **1995**, *5*, 1649−1669.
(27) Shearman, G. C.; Ces, O.; Templer, R. H. Towards an Understanding of Phase Transitions between Inverse Bicontinuous Cubic Lyotropic Liquid Crystalline Phases. *Soft Matter* **2010**, *6*, 256−262.
(28) Kulkarni, C. V.; Tang, T.-Y.; Seddon, A. M.; Seddon, J. M.; Ces, O.; Templer, R. H. Engineering Bicontinuous Cubic Structures at the Nanoscale-The Role of Chain Splay. *Soft Matter* **2010**, *6*, 3191−3194.
(29) Shearman, G. C.; Ces, O.; Templer, R. H.; Seddon, J. M. Inverse Lyotropic Phases of Lipids and Membrane Curvature. *J. Phys.: Condens. Matter* **2006**, *18*, S1105.
(30) Templer, R. H.; Seddon, J. M.; Warrender, N. A.; Syrykh, A.; Huang, Z.; Winter, R.; Erbes, J. Inverse Bicontinuous Cubic Phases in 2:1 Fatty Acid/Phosphatidylcholine Mixtures. The Effects of Chain Length, Hydration, and Temperature. *J. Phys. Chem. B* **1998**, *102*, 7251−7261.
(31) Shearman, G. C.; Khoo, B. J.; Motherwell, M.-L.; Brakke, K. A.; Ces, O.; Conn, C. E.; Seddon, J. M.; Templer, R. H. Calculations of and Evidence for Chain Packing Stress in Inverse Lyotropic Bicontinuous Cubic Phases. *Langmuir* **2007**, *23*, 7276−7285.
(32) Anderson, D. M.; Gruner, S. M.; Leibler, S. Geometrical Aspects of the Frustration in the Cubic Phases of Lyotropic Liquid Crystals. *Proc. Natl. Acad. Sci. U.S.A.* **1988**, *85*, 5364−5368.
(33) Cui, W.; Li, F.; Allinger, N. L. Simulation of Conformational Dynamics with the MM3 Force Field: The Pseudorotation of Cyclopentane. *J. Am. Chem. Soc.* **1993**, *115*, 2943−2951.
(34) Eliel, E. L.; Wilen, S. H. *Stereochemistry of Organic Compounds*; Wiley: New York, 1994.
(35) Ruiz de Ballesteros, O.; Cavallo, L.; Auriemma, F.; Guerra, G. Conformational Analysis of Poly(Methylene-1,3-Cyclopentylene) and Chain Conformation in the Crystalline Phase. *Macromolecules* **1995**, *28*, 7355−7362.
(36) Cherezov, V.; Clogston, J.; Papiz, M. Z.; Caffrey, M. Room to Move: Crystallizing Membrane Proteins in Swollen Lipidic Mesophases. *J. Mol. Biol.* **2006**, *357*, 1605−1618.
(37) Shah, J. C.; Sadhale, Y.; Chilukuri, D. M. Cubic Phase Gels as Drug Delivery Systems. *Adv. Drug Delivery Rev.* **2001**, *47*, 229−250.
(38) Landau, E. M.; Rosenbusch, J. P. Lipidic Cubic Phases: A Novel Concept for the Crystallization of Membrane Proteins. *Proc. Natl. Acad. Sci. U.S.A.* **1996**, *93*, 14532−14535.
(39) Negrini, R.; Mezzenga, R. pH-Responsive Lyotropic Liquid Crystals for Controlled Drug Delivery. *Langmuir* **2011**, *27*, 5296−5303.
(40) Conn, C. E.; Mulet, X.; Moghaddam, M. J.; Darmanin, C.; Waddington, L. J.; Sagnella, S. M.; Kirby, N.; Varghese, J. N.; Drummond, C. J. Enhanced Uptake of an Integral Membrane Protein, the Dopamine D2l Receptor, by Cubic Nanostructured Lipid

Nanoparticles Doped with Ni(II) Chelated Edta Amphiphiles. *Soft Matter* **2011**, *7*, 567−578.
(41) Yaghmur, A.; Glatter, O. Characterization and Potential Applications of Nanostructured Aqueous Dispersions. *Adv. Colloid Interface Sci.* **2009**, *147*−*148*, 333−342.
(42) Fraser, S. J.; Rose, R.; Hattarki, M. K.; Hartley, P. G.; Dolezal, O.; Dawson, R. M.; Separovic, F.; Polyzos, A. Preparation and Biological Evaluation of Self-Assembled Cubic Phases for the Polyvalent Inhibition of Cholera Toxin. *Soft Matter* **2011**, *7*, 6125−6134.